

# **Precision spectroscopy of iodine absorption lines near the $^1S_0$ - $^3P_2$ transition of Yb atoms at 507 nm**

Yuma Sakamoto, Yujin Kawai, Daisuke Akamatsu, and Feng-Lei Hong\*

*Department of Physics, Graduate School of Engineering Science, Yokohama National University, 79-5 Tokiwadai, Hodogaya-ku, Yokohama 240-8501, Japan*

E-mail: hong-feng-lei-mt@ynu.ac.jp

We performed Doppler-free spectroscopy on the P(40)52-0 and P(52)53-0 lines of molecular iodine ( $^{127}\text{I}_2$ ) near the  $^1S_0$ - $^3P_2$  metastable transition of Yb at 507 nm. The frequency instability of an external-cavity diode laser locked to the observed hyperfine transitions of the  $^{127}\text{I}_2$  lines reached a level below  $1.0 \times 10^{-12}$ , at the average time  $\tau$  of the measurement of  $>10$  s. The absolute frequency of the laser locked to the hyperfine transitions was measured with an uncertainty of 8 kHz (fractionally  $1.4 \times 10^{-11}$ ) using an optical frequency comb. The hyperfine transition intervals were fitted to a four-term Hamiltonian to validate the measurements and calculate the hyperfine constants of the iodine lines. The observed 30 hyperfine transitions of the P(40)52-0 and P(52)53-0 lines of  $^{127}\text{I}_2$  can be used as optical frequency references to investigate the  $^1S_0$ - $^3P_2$  transition of Yb atoms.

## 1. Introduction

Optical frequency metrology is of significant interest for precisely measuring time and length and in industrial applications, including broadband communication networks and navigation.<sup>1)</sup> In physics experiments, laser frequency control and measurement are the key technologies investigating cold atoms, which are used to realize optical clocks,<sup>2)</sup> quantum simulation,<sup>3)</sup> and quantum information processing.<sup>4)</sup>

For Yb atoms, the  $^1S_0$ - $^3P_2$  metastable transition at 507 nm has a natural linewidth of approximately 10 mHz<sup>5)</sup> and is suitable for precision measurements and quantum computations. The first example of precision measurement using Yb atoms was the isotope-shift measurement for the King plot study.<sup>6)</sup> In the King plot study, isotope shifts of two different electronic transitions were precisely measured, and their linear relation (King plot linearity) was investigated to search for new physics. Recently, King plots have been constructed using the  $^1S_0$ - $^3P_0$  ultranarrow optical clock transition in Yb and two optical transitions in  $Yb^+$  for the search for new Boson.<sup>7)</sup> High-resolution spectroscopy and precision isotope-shift measurement of the ultranarrow  $^1S_0$ - $^3P_2$  transition should further improve King plots or construct a higher-dimensional King plot.<sup>7)</sup> Another example of precision measurement using Yb atoms is high-resolution laser spectroscopy of a Bose–Einstein condensate (BEC) using the magnetic quadrupole  $^1S_0$ - $^3P_2$  transition.<sup>8)</sup> This method has been used to evaluate the inhomogeneous density distribution and inter-atomic interaction in Yb BEC.<sup>8)</sup> Finally, a scalable quantum computer has been proposed using the  $^1S_0$ - $^3P_2$  transition of Yb atoms in an optical lattice.<sup>9)</sup> In this scheme, two different types of qubits were considered: one composed of the nuclear spin 1/2 for memory (the ground state  $^1S_0$ ) and the other of the electron spin for a gate operation (the metastable state  $^3P_2$ ).<sup>9)</sup>

In all these experiments, an optical reference at 507 nm near the  $^1S_0$ - $^3P_2$  transition was extremely useful for stabilizing the laser source for atom manipulation or calibrating frequency in spectroscopy. Typically, an optical frequency comb is used as the frequency reference. However, an optical frequency comb is complicated and expensive. A frequency-stabilized laser based on sub-Doppler spectroscopy of atomic or molecular transitions near 507 nm should provide an alternative frequency reference with a simple setup and cost efficiency. Furthermore, a frequency-stabilized laser based on atomic or molecular transitions provides an absolute frequency that can be used to recognize the mode number of an optical frequency comb or to measure the frequency drift of a high-finesse optical cavity. An example was demonstrated by measuring the zero-cross temperature of a high-finesse ultralow expansion (ULE) cavity using saturation spectroscopy of  $^{127}I_2$  at 507 nm.<sup>10)</sup>

High-precision spectroscopy of  $^{127}\text{I}_2$  near 507 nm is also attractive for studying molecular iodine. The molecular iodine spectrum covers the wavelength range from green to near-infrared, with the maximum intensity in the green wavelength region. Furthermore, the natural linewidth of the iodine lines near 500 nm was found to be narrower than that of the other lines, with the narrowest natural linewidth of approximately 43 kHz at 508 nm.<sup>11)</sup> Although precision spectroscopy and laser frequency measurements have been performed at 532 nm<sup>12-14)</sup> and 515 nm,<sup>15-17)</sup> only a few researchers have investigated molecular iodine in the wavelength region of <510 nm. Doppler-free spectroscopy and hyperfine structure measurements were demonstrated for  $^{127}\text{I}_2$  at 501 nm with an uncertainty of 18 kHz.<sup>15)</sup> At 507 nm, Doppler-free spectroscopy and hyperfine splitting measurement were performed for the P(40)52-0 line with an uncertainty of 0.7 MHz.<sup>10)</sup> However, the absolute frequencies of the hyperfine transitions were not measured.<sup>10)</sup>

In this paper, we demonstrate the Doppler-free spectroscopy of two relatively strong iodine lines, the P(40)52-0 and P(52)53-0 lines at 507 nm, near the  $^1\text{S}_0$ - $^3\text{P}_2$  transition of Yb. Laser frequency was stabilized using the observed Doppler-free hyperfine transitions in the iodine lines. The frequency instability was evaluated to be below 0.59 kHz ( $1.0 \times 10^{-12}$ ) when the average time  $\tau$  of the measurement was >10 s. The absolute frequency of each hyperfine transitions of the lines was measured with an uncertainty of 8 kHz (fractionally  $1.4 \times 10^{-11}$ ) using an optical frequency comb. The hyperfine structures of the two lines were measured and theoretically fitted with an uncertainty of 3–6 kHz. Consequently, the observed 30 hyperfine transitions in the iodine lines provided useful frequency references for research using the  $^1\text{S}_0$ - $^3\text{P}_2$  transition of Yb atoms.

## 2. Experimental setup

Figure 1 shows a schematic of the experimental setup for the Doppler-free spectroscopy and absolute frequency measurement of the iodine lines at 507 nm. A homemade external-cavity diode laser (ECDL) at 1014 nm was used as the light source. The ECDL contained a laser diode (TOPTICA, EYP-RWE-1060-10525-1500-SOT02-0000) with a Littrow configuration. The ECDL output was fed to a semiconductor optical amplifier (SOA) (Innolume: SOA-1020-110-PM-27 dB) for power amplification. The SOA output was injected into a periodically poled lithium niobate waveguide (PPLN-WG) for second-harmonic generation (SHG) at 507 nm. The free-space light from the PPLN-WG was separated into the fundamental and SHG laser beams using a dichroic mirror. The SHG laser beam was sent to an iodine spectrometer for Doppler-free spectroscopy and laser-frequency stabilization. The

iodine spectrometer was equipped with an optical fiber at its entrance. The switching of the SC connector at the end of the optical fiber facilitates switching between different light sources for the spectrometer. Doppler-free spectroscopy of molecular iodine is based on saturation spectroscopy using the modulation transfer technique.<sup>18,19)</sup> The iodine spectrometer was similar to that used in our previous study, related to the precision spectroscopy of iodine lines near the  $^1S_0$ - $^3P_1$  transition of Yb atoms at 556 nm.<sup>20)</sup> Here, we have provided a simple description of the arrangement inside the spectrometer. The SHG light was split into pump and probe beams using a half-wave plate and polarizing beam splitter. The pump beam was frequency shifted by 80 MHz using an acousto-optic modulator (AOM) and then phase-modulated at 350 kHz using an electro-optic modulator (EOM). The pump was then injected into a 45-cm iodine cell overlapping anticollinearly with the probe beam. The sidebands of the pump light were transferred to the probe light via a four-wave mixing process when saturation absorption occurs.<sup>18,19)</sup> The probe beam that passed through the iodine cell was reflected by a Glan-Thompson polarizer and detected using a photodetector (PD1). The detected signal was demodulated using a double-balanced mixer and signal from a local oscillator, the phase of which was offset from the signal applied to the EOM. The demodulated signal was used as an error signal for servo control of the laser frequency via the piezoelectric transducer of the ECDL. The fundamental laser beam was sent to an optical frequency comb for beat-frequency measurements. The optical frequency comb was an erbium-doped fiber comb with an iodine-stabilized Nd:YAG laser as the frequency reference.<sup>21)</sup> The beat signal observed by the photodetector (PD2) was measured using a dead-time-free frequency counter (Pendulum: CNT-91).

### 3. Results

#### 3.1 Doppler-free spectroscopy of molecular iodine

Figure 2 shows the frequency relationship between the  $^1S_0$ - $^3P_2$  transition of the six stable isotopes of Yb (indicated as blue lines in the figure)<sup>22)</sup> and nearby iodine absorption lines.<sup>23)</sup> The absolute frequencies of the  $^{176}\text{Yb}$ ,  $^{173}\text{Yb}$ ,  $^{172}\text{Yb}$ ,  $^{171}\text{Yb}$ , and  $^{170}\text{Yb}$  isotopes were estimated from other transitions involving the  $^3P_2$  state with an uncertainty of tens of MHz, whereas that of the  $^{174}\text{Yb}$  isotope was measured directly at the  $^1S_0$ - $^3P_2$  transition with an uncertainty of tens of kHz.<sup>22)</sup> For comparison, the nearby iodine lines measured using Doppler-limited spectroscopy with an uncertainty of GHz<sup>23)</sup> are also shown in Fig. 2 as green solid lines.

Figures 3(a) and 3(b) show the hyperfine structures of the P(40)52-0 and P(52)53-0 lines observed using the Doppler-free modulation transfer technique.<sup>18,19)</sup> The laser frequency was

scanned by continuously tuning the temperature of the laser. The iodine pressure inside the cell was 4.0 Pa. The optical powers of the pump and probe beams were 2.0 and 0.3 mW, respectively. The laser beam diameter was 0.7 mm. All the 15 hyperfine transitions were resolved in the observed modulation transfer signal. In the P(40)52-0 line, weak signals were detected near the  $a_1$  hyperfine transition and were assigned to the hyperfine transitions of the R(16)61-1 line.<sup>22)</sup> The signal-to-noise ratio (S/N), recorded using a low-pass filter with a bandwidth of 100 Hz, for the  $a_1$  hyperfine transition of the P(52)53-0 line was 276.

### 3.2 Frequency stability and repeatability

The laser frequency was stabilized using the observed  $a_1$  hyperfine transition of the P(52)53-0 line. In laser frequency locking, the locking quality was limited by the S/N of the observed spectrum. The red solid curve with solid circles in Fig. 4(a) shows the Allan standard deviation calculated from the measured beat frequency between the frequency-stabilized laser and optical frequency comb. The Allan standard deviation was  $2.9 \times 10^{-12}$  at the average time  $\tau = 1$  s, decreasing to  $4.3 \times 10^{-13}$  at  $\tau = 100$  s and kept to  $< 1.0 \times 10^{-12}$  until  $\tau = 10000$  s. For comparison, the frequency instability of the optical frequency comb is also shown in Fig. 4(a) as a black dashed line.<sup>21)</sup> As the frequency comb is more stable than the developed iodine-stabilized laser, the observed Allan standard deviation (red solid curve with solid circles) indicated instability of the developed laser. The solid blue curve with solid circles in Fig. 4(a) represents the free-running frequency instability of the ECDL. The frequency stability of the locked laser was improved by approximately three orders and more than four orders of magnitude at  $\tau = 1$  and 100 s, respectively.

Figure 4(b) shows the frequency measurement results of the laser locked to the  $a_1$  hyperfine transition of the P(52)53-0 line. Thirteen frequency measurements were recorded over three days. Each measurement was recorded from 600 beat frequency data points measured with a gate time of 1 s. The uncertainty bar in this figure considered the Allan standard deviation at the longest averaging time, which was calculated using each set of 600 beat frequency data points. The averaged frequency of the 13 measurements was 590 903 990 563.3 kHz. The standard deviation of the 13 measurements was 0.6 kHz, indicating the repeatability of the developed laser.

### 3.3 Uncertainty evaluation

To evaluate the systematic uncertainty of the measured frequency, we investigated the effects of frequency shift of the iodine-stabilized laser (Table I). The pressure shift

sensitivity was measured to be  $-1.7(0.4)$  kHz/Pa (Fig. 5(a)). The uncertainty of the iodine pressure was estimated to be  $<0.2$  Pa, resulting in a frequency uncertainty of  $<0.34$  kHz. The laser power shift sensitivity was measured to be  $-4.1(0.4)$  kHz/mW (Fig. 5(b)). As the uncertainty in the determination of the pump power was  $<5\%$ , the frequency uncertainty was estimated to be  $<0.41$  kHz. The sensitivity of the frequency shift due to the EOM phase adjustment in the demodulation process was measured to be  $0.05$  kHz/deg. As the uncertainty of the phase adjustment was set to  $<20^\circ$ , the corresponding frequency uncertainty was  $<1.0$  kHz. The sensitivity of the frequency shift owing to the servo electronic offset was measured to be  $0.65$  kHz/mV. In this experiment, the offset voltage was carefully adjusted to an uncertainty of  $<2$  mV, resulting in a frequency uncertainty of  $<1.3$  kHz.

Figure 6(a) shows the frequency shift owing to the misalignment of the pump and probe beams, where multiple alignment optimizations (alignment changes by different people) were tested to maximize the modulation transfer signal. The frequency uncertainty owing to the misalignment was estimated to be  $5.9$  kHz using the standard deviation of the measurement, as shown in Fig. 5(a). The uncertainty of the cell impurity ( $5$  kHz) is provided in the CIPM recommendation.<sup>24)</sup> The uncertainty of the frequency reference used in the frequency comb, calculated from the repeatability of the iodine-stabilized Nd:YAG laser, was  $0.3$  kHz. By combining these uncertainties with the statistical uncertainty, the total uncertainty of the absolute frequency measurement in this study was estimated to be  $8.0$  kHz (relatively  $1.4 \times 10^{-11}$ ).

As listed in Table I, the frequency uncertainty due to the misalignment of the pump and probe beams is the largest item in the systematic uncertainty budget. In this experiment, the laser-beam diameter was  $0.7$  mm. This relatively small beam diameter caused a relatively large frequency shift during the laser beam alignment. In our previous experiment on precision iodine spectroscopy at  $556$  nm,<sup>20)</sup> the beam diameter was  $1.2$  mm, and the associated frequency uncertainty was  $3.7$  kHz. The small beam diameter used in the present experiment was associated with the intensity noise of the laser beam. Figure 6(b) shows the measured intensity noise of the  $507$  and  $556$  nm laser beams with blue and green curves, respectively. For comparison, the red curve shows the shot noise level. A peak close to  $310$  kHz in the intensity noise of the laser beams was caused by the SOA controller (confirmed by the manufacturer). The modulation frequency of  $350$  kHz used in the present experiment was off-peak noise. However, the intensity noise level of the  $507$  nm laser beam was approximately  $5$  dB higher than that of the  $556$  nm laser beam. This higher-intensity noise increased the noise and hence reduced the S/N in the modulation transfer spectrum. This

degraded the laser frequency stability. The higher intensity noise observed in the 507 nm laser beam was caused by the SOA and increased with the SOA gain. To reduce the noise intensity and achieve saturation spectroscopy with a relatively small laser power, we limited the output power of the SOA and reduced the laser beam diameter in the iodine spectrometer.

### 3.4 Absolute frequency and hyperfine structure

The measured absolute frequencies of the laser locked to the  $a_1$  hyperfine transitions of the P(40)52-0 and P(52)53-0 lines are listed in Table II. The frequency of the  $a_1$  hyperfine transition of the P(52)53-0 line was derived from the measurements shown in Fig. 4(b). The frequency of the  $a_1$  hyperfine transition of the P(40)52-0 lines was measured using the average beat frequency data for 600 s. The frequencies were directly measured under the experimental conditions described in Section 3.1.

To measure the hyperfine splitting, the iodine-stabilized laser was locked sequentially to all 15 hyperfine transitions of the P(40)52-0 and P(52)53-0 lines. The frequency of each hyperfine transition was measured for over 600 s. The values in the columns “Obs.” in Table III are the measured hyperfine splittings of the two iodine lines, obtained by taking the frequency difference between each hyperfine and  $a_1$  transitions. As the frequency shift is similar for each hyperfine transition, the systematic uncertainties do not affect the measurement uncertainty of the hyperfine splitting interval. The measurement uncertainty of the hyperfine splitting is limited by the repeatability of the developed iodine-stabilized laser.

The measured intervals of the hyperfine transitions were fitted to a four-term Hamiltonian<sup>15)</sup> to validate the measurements and calculate the hyperfine constants of the iodine lines. The four-term Hamiltonian includes the electric quadrupole, spin-rotation, tensor spin-spin, and scalar spin-spin interactions, where  $eQq$ ,  $C$ ,  $d$ , and  $\delta$  are the respective hyperfine constants corresponding these interactions.<sup>15)</sup> In the present calculation, a nonlinear least-squares fit was performed using the ROOT analysis libraries of CERN.<sup>25)</sup> The detailed procedure and parameters of the fitting are described elsewhere.<sup>26,27)</sup> The calculated hyperfine splittings from the fit are listed in the columns “Cal.” in Table III. The standard deviations of the theoretical fit were 3.4 and 6.1 kHz for the P(40)52-0 and P(52)53-0 lines, respectively. Thus, the hyperfine splitting measurement of the iodine lines was verified at the kilohertz level using a theoretical fit. The standard deviation of the fit of the P(52)53-0 line was approximately twice that of the P(40)52-0 line. In the visible wavelength region, the iodine lines with different absorption strengths often overlap. The larger standard deviation of the fit for the P(52)53-0 line maybe caused by some weak lines overlapping

with the P(52)53-0 line. Through the theoretical fit, hyperfine constants  $\Delta eQq$ ,  $\Delta C$ ,  $\Delta d$ , and  $\Delta\delta$ , which are the differences in the hyperfine constants between the upper and lower states, can be obtained. The calculated hyperfine constants of the two lines are listed in Table IV.

#### 4. Discussion and Conclusions

The observed 30 hyperfine transitions of the two iodine lines examined in this study can be used as frequency references for further research on Yb atoms. For example, we investigated the frequency references suitable for the  $^{174}\text{Yb}$  and  $^{171}\text{Yb}$  isotopes. The  $^{174}\text{Yb}$  isotope has the highest natural abundance (32 %) among all isotopes and is often used to investigate Bose-Einstein condensation.<sup>28)</sup> The  $^{171}\text{Yb}$  isotope has a reasonable natural abundance of 14 %, a relatively simple nuclear spin system ( $I = 1/2$ ), and is used in optical lattice clocks.<sup>29)</sup> The frequencies of the  $^1\text{S}_0$ - $^3\text{P}_2$  transitions of  $^{174}\text{Yb}$  and  $^{171}\text{Yb}$  are listed in Table II for comparison.<sup>22)</sup> From the data in Table II and III, the frequency of the  $a_{15}$  hyperfine transition of the P(40)52-0 line was found to be approximately 193 MHz lower than that of the  $^1\text{S}_0$ - $^3\text{P}_2$  transition of the  $^{174}\text{Yb}$  isotope. In addition, the frequency of the  $a_5$  hyperfine transition of the P(52)53-0 line was approximately 4 MHz higher than that of the  $^1\text{S}_0$ - $^3\text{P}_2$  transition of the  $^{171}\text{Yb}$  isotope. The hyperfine transitions of the iodine lines close to the Yb transitions are shown in the inset of Fig. 2 as dashed green lines. Frequency separation can be easily bridged using offset locking or an AOM.

The instantaneous linewidth of the iodine-stabilized laser was measured using a frequency comb.<sup>21)</sup> The inset of Fig. 4(a) shows the observed beat signal between the fundamental beam of the frequency-stabilized laser and comb component. The resolution bandwidth and sweep time of the spectrum analyzer were 3 kHz and 1.5 s, respectively. The observed linewidth was approximately 60 kHz, corresponding to 120 kHz at 507 nm. This was mainly attributed to the linewidth of the developed iodine-stabilized laser, as the linewidth of the frequency comb was in the kilohertz range. Although the observed iodine hyperfine transitions can be used as frequency references, the linewidth of the iodine-stabilized laser needs to be further improved (linewidth narrowing) for research on the ultranarrow  $^1\text{S}_0$ - $^3\text{P}_2$  transition.

We obtained highly accurate hyperfine constants  $\Delta eQq$ ,  $\Delta C$ ,  $\Delta d$ , and  $\Delta\delta$  for the P(40)52-0 and P(52)53-0 lines of  $^{127}\text{I}_2$ . Accurate hyperfine constants are necessary to reproduce or simulate the hyperfine spectrum of iodine. Therefore, theoretical models for predicting hyperfine constants are essential in spectroscopy.<sup>30)</sup> In our previous work, we derived formulae to express the rotation dependence of the ground state  $eQq'$  ( $v' = 0$ )<sup>31)</sup> and excited states  $eQq'$  ( $v' = 32$  and  $44$ ).<sup>27,32,33)</sup> The hyperfine constants obtained in this study can be

used to improve our understanding of the rotation dependence of the excited state hyperfine constants for  $\nu' = 52$  and 53.

In conclusion, we studied the hyperfine structure of two absorption lines of molecular iodine, the P(40)52-0 and P(52)53-0 lines near the 507 nm transition of Yb. All hyperfine transitions in these lines were observed using the sub-Doppler modulation transfer technique. The absolute frequency of each transition was measured using an optical frequency comb. The 30 hyperfine transitions of the two iodine lines studied in this work are close to the  $^1S_0$ - $^3P_2$  metastable transition and can be used as frequency references for research on Yb atoms.

## Acknowledgments

This study was supported by the Japan Society for the Promotion of Science (JSPS) KAKENHI 18H03886 and the Japan Science and Technology Agency (JST) Moonshot R&D (Grant Number JPMJMS226C). The authors would like to thank T. Kobayashi for helpful discussions on the calculation of hyperfine splittings and S. Matsunaga, S. Aoyama, and R. Takeda for their technical assistance with the experiments.

## References

- 1) F.-L. Hong, Meas. Sci. Technol. **28**, 012002 (2016).
- 2) M. Takamoto, F.-L. Hong, R. Higashi, and H. Katori, Nature **435**, 321 (2005).
- 3) F. Schäfer, T. Fukuhara, S. Sugawa, Y. Takasu, and Y. Takahashi, Nat. Rev. Phys. **2**, 411 (2020).
- 4) A. Daley, Quantum Inf. Proc. **10**, 865 (2011).
- 5) A. P. Mishra and T. K. Balasubramanian, J. Quant. Spectrosc. Radiat. Transf. **69**, 769 (2001).
- 6) W. H. King, J. Opt. Soc. Am. **53**, 638 (1963).
- 7) K. Ono, Y. Saito, T. Ishiyama, T. Higomoto, T. Takano, Y. Takasu, Y. Yamamoto, M. Tanaka, and Y. Takahashi, Phys. Rev. X **12**, 021033 (2022).
- 8) A. Yamaguchi, S. Uetake, S. Kato, H. Ito, and Y. Takahashi, New J. Phys. **12**, 103001 (2010).
- 9) K. Shibata, S. Kato, A. Yamaguchi, S. Uetake, and Y. Takahashi, Appl. Phys. B **97**, 753 (2009).
- 10) I. Shomura, Graduation thesis, Kozuma-lab, Tokyo Institute of Technology [in Japanese]. <http://www.kozuma.phys.titech.ac.jp/shomura.pdf>
- 11) W.-Y. Cheng, L. Chen, T. H. Yoon, J. L. Hall, and J. Ye, Opt. Lett. **27**, 571 (2002).
- 12) A. Arie and R. L. Byer, J. Opt. Soc. Am. B **10**, 1990 (1993).
- 13) M. L. Eickhoff and J. L. Hall, IEEE Trans. Instrum. Meas. **44**, 155 (1995).
- 14) F.-L. Hong and J. Ishikawa, Opt. Commun. **183**, 101 (2000).
- 15) Ch. J. Bordé, G. Camy, B. Decomps, J.-P. Descoubes, and J. Vigué, J. Phys. (Paris) **42**, 1393 (1981).
- 16) J. P. Wallerand, L. Robertson, L.-S. Ma, and M. Zucco, Metrologia **43**, 294 (2006).
- 17) K. Ikeda, S. Okubo, M. Wada, K. Kashiwagi, K. Yoshii, H. Inaba, and F.-L. Hong, Opt. Express **28**, 2166 (2020).
- 18) J. H. Shirley, Opt. Lett. **7**, 537 (1982).
- 19) G. Camy, Ch. J. Bordé, and M. Ducloy, Opt. Commun. **41**, 325 (1982).
- 20) Y. Tanabe, Y. Sakamoto, T. Kohno, D. Akamatsu, and F.-L. Hong, Opt. Express **30**, 46487 (2022).
- 21) Y. Asahina, K. Yoshii, Y. Yamada, Y. Hisai, S. Okubo, M. Wada, H. Inaba, T. Hasegawa, Y. Yamamoto, and F.-L. Hong, Jpn. J. Appl. Phys. **58**, 038003 (2019).
- 22) A. Yamaguchi, “Metastable State of Ultracold and Quantum Degenerate Ytterbium Atoms: High-Resolution Spectroscopy and Cold Collisions,” PhD thesis, Kyoto

- University (2008). [http://yagura.scphys.kyoto-u.ac.jp/publications/thesis/PhD\\_yamaguchi.pdf](http://yagura.scphys.kyoto-u.ac.jp/publications/thesis/PhD_yamaguchi.pdf)
- 23) S. Gerstenkorn and P. Luc, “Atlas du Spectre d’Absorption de la Molecule d’Iode,” Editions de CNRS, Paris (1978).
  - 24) <https://www.bipm.org/en/publications/mises-en-pratique/standard-frequencies.html>
  - 25) R. Brun and F. Rademakers, Nucl. Instrum. Methods Phys. Res., Sect. A **389**, 81 (1997).
  - 26) T. Kobayashi, D. Akamatsu, K. Hosaka, H. Inaba, S. Okubo, T. Tanabe, M. Yasuda, A. Onae, and F.-L. Hong, J. Opt. Soc. Am. B **33**, 725 (2016).
  - 27) H. Sakagami, K. Yoshii, T. Kobayashi, and F.-L. Hong, J. Opt. Soc. Am. B **37**, 1027 (2020).
  - 28) Y. Takasu, K. Maki, K. Komori, T. Takano, K. Honda, M. Kumakura, T. Yabuzaki, and Y. Takahashi, Phys. Rev. Lett. **91**, 040404 (2003).
  - 29) T. Kohno, M. Yasuda, K. Hosaka, H. Inaba, Y. Nakajima, and F.-L. Hong, Appl. Phys. Express **2**, 072501 (2009).
  - 30) B. Bodermann, H. Knöckel, E. Tiemann, Eur. Phys. J. D **19**, 31 (2002).
  - 31) F.-L. Hong, J. Ye, L.-S. Ma, S. Picard, Ch. J. Bordé, and J. L. Hall, J. Opt. Soc. Am. B **18**, 379 (2001).
  - 32) F.-L. Hong, J. Ishikawa, A. Onae, and H. Matsumoto, J. Opt. Soc. Am. B **18**, 1416 (2001).
  - 33) M. Yoshiki, S. Matsunaga, K. Ikeda, D. Akamatsu, and F.-L. Hong, Eur. Phys. J. D **77**, 140 (2023).

## Figure Captions

**Fig. 1.** Diagram of the experimental setup. ECDL: external cavity diode laser, SOA: semiconductor optical amplifier, PPLN-WG: periodically poled lithium niobate waveguide, DM: dichroic mirror, SC: subscriber connector, HWP: half-wave plate, PBS: polarizing beam splitter, AOM: acousto-optic modulator, EOM: electro-optic modulator, TEC: thermoelectric cooler, GTP: Glan-Thompson polariser, PD: photodetector, DBM: double-balanced mixer, LO: local oscillator, Nd:YAG/I2: iodine-stabilized Nd:YAG laser.

**Fig. 2.** Frequency atlas of the  $^{127}\text{I}_2$  absorption lines near the  $^1\text{S}_0\text{-}^3\text{P}_2$  transition of Yb at 507 nm. The  $^1\text{S}_0\text{-}^3\text{P}_2$  transition of six isotopes of Yb are also indicated.<sup>22)</sup> The relative intensity of iodine lines was taken from Ref. 23. The intensity of the Yb double-forbidden transition is not on the same scale with the iodine lines. The insets indicate the relationship of two observed hyperfine transitions located near the  $^{174}\text{Yb}$  and  $^{171}\text{Yb}$  isotopes.

**Fig. 3.** Observed hyperfine structures of P(40)52-0 and P(52)53-0 lines of  $^{127}\text{I}_2$  near 507 nm. The low pass filter for recording had a bandwidth of 100 Hz. Vertical scales are the same for all graphs.

**Fig. 4.** (a) Allan standard deviations calculated from the beat frequency of the iodine-stabilized 1014 nm ECDL and the optical frequency comb (red solid curve with solid circles). The instabilities of the frequency comb (black dashed line) are shown for comparison. The blue solid curve with solid circles is the measured free-running frequency instability of the 1014 nm ECDL. The inset indicates the beat signal between the fundamental light of the frequency-stabilized laser and frequency comb, measured using a spectrum analyzer. The observed linewidth from the beat measurement was approximately 60 kHz (corresponding to 120 kHz at 507 nm). (b) Measured absolute frequency of the laser locked on the  $a_1$  hyperfine transition of the P(52)53-0 line. The red line represents the average frequency of 13 measurements recorded on different days.

**Fig. 5.** Frequency shift of the iodine-stabilized laser. (a) Pressure shift, (b) power shift.

**Fig. 6.** (a) Frequency shift due to the misalignment of the pump and probe beams. The red line represents the average frequency of 11 measurements. (b) Intensity noise of the 507 and 556 nm laser beams indicated using blue and green curves, respectively. The red curve indicates the shot noise level.

**Table I.** Frequency shift

Effect	Sensitivity	Uncertainty
Pressure shift	-1.7 kHz/Pa	< 0.34 kHz
Power shift	-4.1 kHz/mW	< 0.41 kHz
EOM phase shift	0.05 kHz/deg	< 1.0 kHz
Offset Voltage	0.65 kHz/mV	< 1.3 kHz
Alignment		5.9 kHz
Cell impurity		5.0 kHz
Frequency reference of the comb		0.3 kHz
Statistics		0.6 kHz
Total uncertainty		8.0 kHz
Relative uncertainty		$1.4 \times 10^{-11}$

**Table II.** Measured absolute frequency of the transitions

Assignment	Frequency
P(40)52-0: $a_1$	590 901 303 762(8) kHz
$^1S_0$ - $^3P_2$ : $^{174}\text{Yb}$	590 902 342 562 (60) kHz*
P(52)53-0: $a_1$	590 903 990 563(8) kHz
$^1S_0$ - $^3P_2$ : $^{171}\text{Yb}$	590 904 326(42) MHz*

\*Ref. 22.

**Table III.** Observed and calculated hyperfine splitting of the three transitions\*

	P(40)52-0			P(52)53-0		
	Obs.	Cal.	Obs.-Cal.	Obs.	Cal.	Obs.-Cal.
$a_1$	0.0	0.1	0.1	0.0	2.2	-2.2
$a_2$	209029.0	209025.4	3.6	182463.3	182455.9	7.4
$a_3$	272768.5	272773.8	-5.3	263912.5	263919.2	-6.6
$a_4$	290179.1	290175.1	4.0	298791.5	298784.4	7.2
$a_5$	352226.1	352228.3	-2.2	339599.6	339602.3	-2.7
$a_6$	357213.0	357216.2	-3.2	373865.4	373867.4	-1.9
$a_7$	387467.1	387468.9	-1.8	378736.0	378744.5	-8.5
$a_8$	454987.5	454984.3	3.2	468853.3	468843.7	9.5
$a_9$	485309.0	485308.2	0.8	502811.5	502808.5	3.0
$a_{10}$	562665.5	562664.4	1.1	562597.8	562599.3	-1.5
$a_{11}$	663518.1	663515.1	3.1	651059.8	651061.7	-1.8
$a_{12}$	678278.7	678280.4	-1.6	673156.7	673161.1	-4.4
$a_{13}$	728186.4	728183.9	2.5	733137.4	733137.3	0.1
$a_{14}$	746289.2	746292.4	-3.2	757861.0	757860.2	0.8
$a_{15}$	845617.8	845618.6	-0.8	845324.8	845323.0	1.8
SD			3.4			6.1

\*All values are in kHz and SD is the standard deviation of the fit.

**Table IV.** Fitted hyperfine constants

Iodine line	P(40)52-0	P(52)53-0
-------------	-----------	-----------

$\Delta eQq$ (kHz)	1885650.6(5.8)	1884987.7(14.1)
$\Delta C$ (kHz)	401.919(10)	446.091(14)
$\Delta d$ (kHz)	-221.56(40)	-245.19(13)
$\Delta \delta$ (kHz)	57.16(49)	79.92(71)

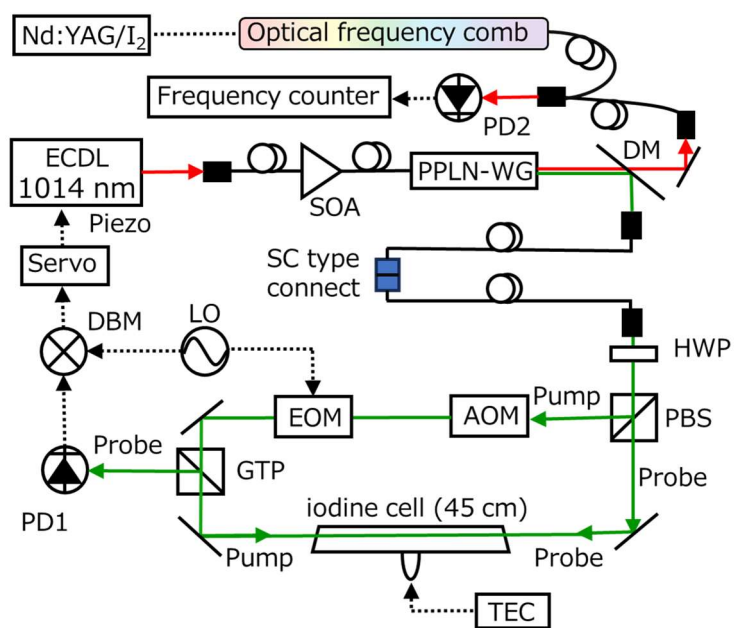


Fig. 1.

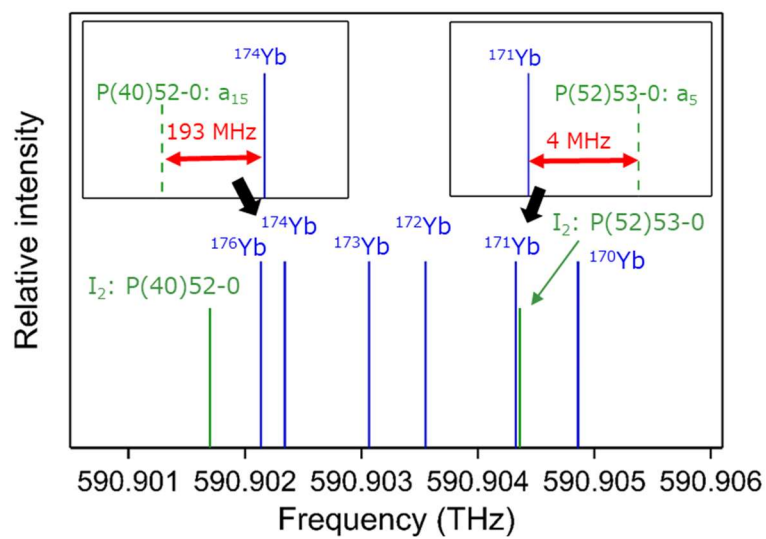


Fig. 2.

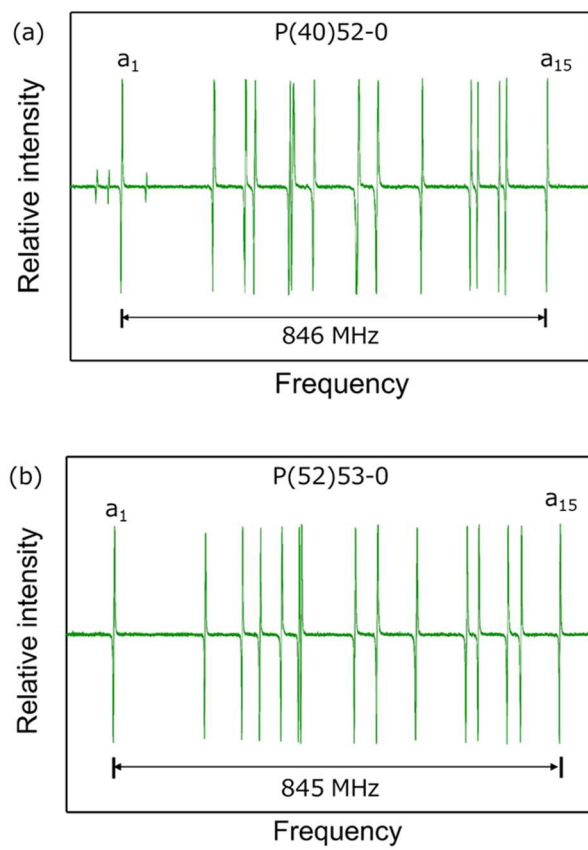


Fig. 3.

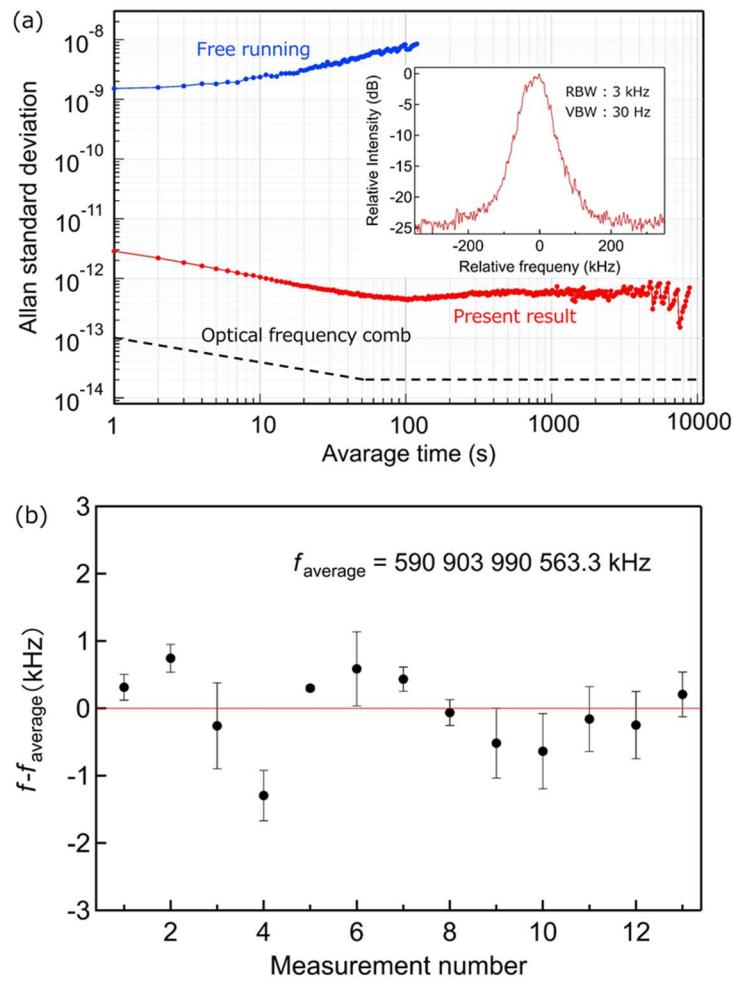


Fig. 4.

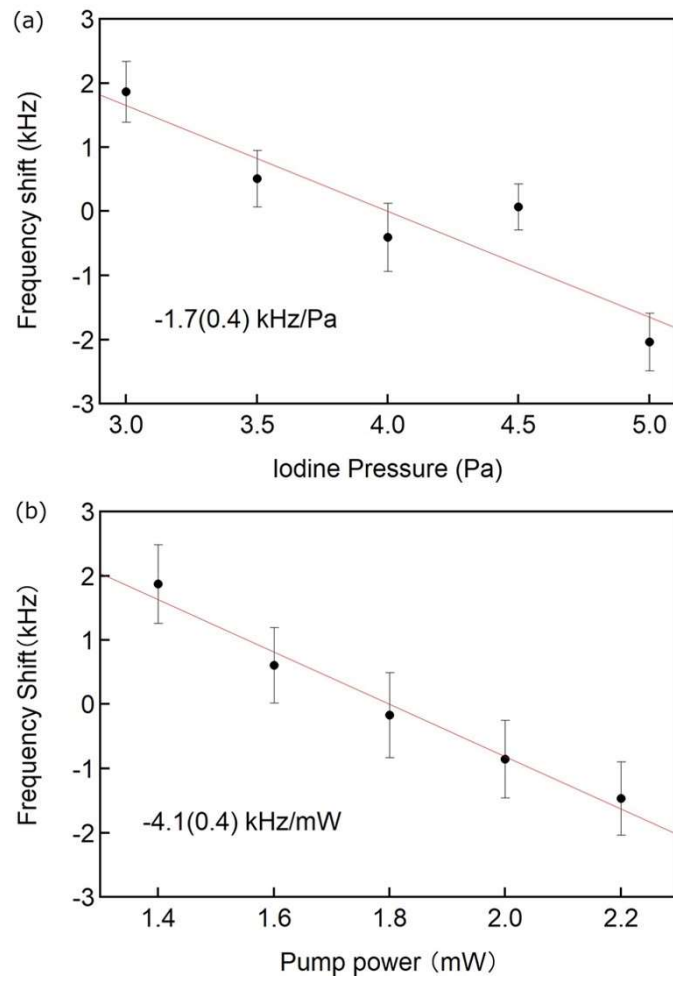


Fig. 5.

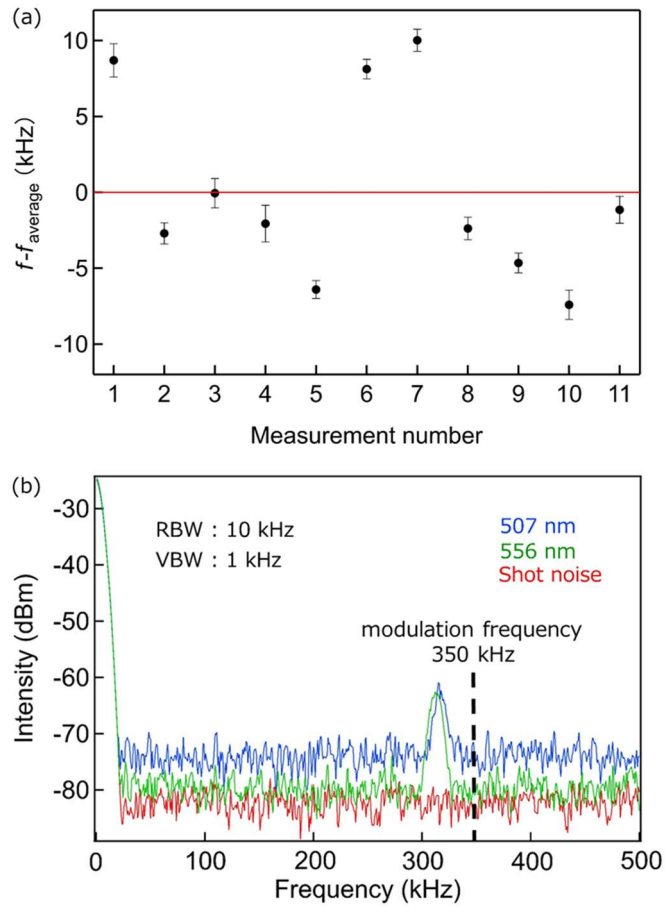


Fig. 6